poultry

MDPI

Article

Electrochemical DNA Biosensor for the Detection of Infectious Bronchitis Virus Using a Multi-Walled Carbon Nanotube-Modified Gold Electrode

Md Safiul Alam Bhuiyan [1,2], Gilbert Ringgit [1], Subir Sarker [3], Ag Muhammad Sagaf Abu Bakar [4], Suryani Saallah [1], Zarina Amin [1], Sharifudin Md. Shaarani [5] and Shafiquzzaman Siddiquee [1,*]

[1] Biotechnology Research Institute, Universiti Malaysia Sabah, Jln UMS, Kota Kinabalu 88400, Sabah, Malaysia; md.safiul@ums.edu.my (M.S.A.B.); gilbertringgit@gmail.com (G.R.); suryani@ums.edu.my (S.S.); zamin@ums.edu.my (Z.A.)
[2] Faculty of Sustainable Agriculture, Livestock Production, University Malaysia Sabah, Locked Bag No. 3, Sandakan 90509, Sabah, Malaysia
[3] Biomedical Sciences & Molecular Biology, College of Medicine and Dentistry, James Cook University, Townsville, QLD 4811, Australia; subir.sarker@jcu.edu.au
[4] Jabatan Perkhidmatan Veterinar Sabah, Makamal Diagnosa Veterinar Kota Kinabalu, Peti Surat No. 59, Tanjung Aru 89457, Sabah, Malaysia; agmuhdsagaf.abubakar@sabah.gov.my
[5] Food Biotechnology Program, Faculty of Science and Technology, Universiti Sains Islam Malaysia, Bandar Baru Nilai, Nilai 71800, Negeri, Malaysia; sharifudinms@usim.edu.my
* Correspondence: shafiqpab@ums.edu.my; Tel.: +60-88320000 (ext. 8467); Fax: +60-88-320993

Abstract: Infectious bronchitis virus (IBV) is an enveloped, positive-sense, single-stranded RNA virus belonging to the genus *Gammacoronavirus*. It primarily infects avian species, causing respiratory and renal disease and irreversible damage to the oviduct, which can lead to high mortality rates in chickens. The lack of rapid and reliable diagnostic tools for on-farm IBV detection hampers timely disease management and control measures. The introduction of DNA biosensors offers a promising approach for the sensitive and specific detection of IBV, facilitating rapid identification and intervention. In this study, an electrochemical DNA biosensor with a multi-walled carbon nanotube (MWCNT)-modified gold electrode was developed for IBV detection. The biosensor targeted the target-specific 5′ untranslated region (5′-UTR) of the IBV genome. Under optimal conditions, the immobilization and hybridization efficiencies were evaluated by cyclic voltammetry (CV) and differential pulse voltammetry (DPV), with methylene blue as a redox indicator. The developed DNA biosensor demonstrated a dynamic detection range from 2.0×10^{-12} to 2.0×10^{-5} mol L^{-1}, with a limit of detection (LOD) of 2.6 nM and a limit of quantification (LOQ) of 0.79 nM. Validation using a small subset of clinical samples, including crude complementary DNA, and polymerase chain reaction products, showed high recovery rates ranging from 95.41% to 99.55%. While these findings highlight the potential of the proposed DNA biosensor as an innovative diagnostic tool for IBV detection, this study remains a proof of concept. However, further validation using a large number of clinical samples is essential to assess its feasibility, robustness, and practical application in a real-world farm setting.

Keywords: IBV; DNA biosensor; voltammetry; chitosan-modified MWCNT

Academic Editor: Vagner Ricardo Lunge

Received: 4 November 2024
Revised: 23 February 2025
Accepted: 3 March 2025
Published: 6 March 2025

Citation: Bhuiyan, M.S.A.; Ringgit, G.; Sarker, S.; Abu Bakar, A.M.S.; Saallah, S.; Amin, Z.; Shaarani, S.M.; Siddiquee, S. Electrochemical DNA Biosensor for the Detection of Infectious Bronchitis Virus Using a Multi-Walled Carbon Nanotube-Modified Gold Electrode. *Poultry* **2025**, *4*, 12. https://doi.org/10.3390/poultry4010012

1. Introduction

Poultry are susceptible to various infectious diseases caused by bacterial, viral, fungal, and parasitic pathogens, which can significantly impact production, welfare, and food

security [1]. Among these, viral diseases pose major challenges due to their rapid spread, high mortality, and potential zoonotic risks [2]. Accurate and early diagnosis is essential for effective disease control, preventing outbreaks, and minimizing economic losses. One of the most economically significant viral diseases in poultry is infectious bronchitis (IB), caused by the infectious bronchitis virus (IBV), a highly contagious coronavirus [3]. The rapid and reliable detection of IBV through molecular assays is crucial for implementing effective control measures [4].

Coronaviruses (CoVs) are a family of enveloped, single-stranded, positive-sense RNA viruses within the order *Nidovirales* that pose a major threat to both animals and humans [5–7]. IBV is a member of the genus *Gammacoronavirus*, mainly affects poultry, and has been a persistent problem since its discovery in 1933. IBV remains a global challenge due to its high infection rate and severe impact on poultry production, with outbreaks causing mortality rates ranging from 10 to 60% in chickens aged 4 to 6 weeks [8,9]. In addition to mortality, IBV induces immunosuppression, which increases susceptibility to secondary infections and leads to significant economic losses [10,11].

Advances in molecular diagnostics over the last three decades, particularly DNA sequencing, have improved the detection and identification of poultry diseases [12,13]. DNA biosensors have shown promise as tools for detecting infectious diseases in animals and humans [14], taking advantage of the high structural integrity of DNA and its affinity for electron transfer [15,16]. However, conventional methods for virus isolation and characterization are labor-intensive, costly, and time-consuming [17,18]. Molecular techniques such as RT-PCR and ELISA provide faster and highly sensitive diagnostics [19] but require pre-amplification steps that carry the risk of contamination and non-linear amplification errors [20,21]. These challenges underline the need for innovative, rapid diagnostic approaches, which were developed in the course of developing an electrochemical DNA biosensor specifically for the detection of IBV, addressing a gap in existing research.

This study represents the advances in nanotechnology that have enabled the development of biosensors with increased sensitivity and efficiency. In addition, this study introduced novel test parameters and a new configuration not previously published in the literature, which were not explored in prior IBV diagnostic studies. This study offers a novel technique for faster and more precise IBV disease management in chicken farms by combining MWCNT, a gold electrode, and methylene blue in an electrochemical DNA biosensor for the 5′-UTR region of the IBV genome. MWCNTs were chosen as an electrode modification material compared to graphene, carbon nanohorns, polyaniline, and gold nanoparticles due to their superior combination of sensitivity, stability, and functionalization potential [22,23]. Together, these nanomaterials improve the detection performance and make this biosensor a highly sensitive and reliable tool for fast and more precise IBV diagnostics [24,25]. The immobilization of single-stranded DNA (ssDNA) probes on electrode surfaces improves biosensor performance through stable alignment and increased hybridization efficiency [26–28]. Here, a biosensor surface with chitosan (CS), MWCNTs, and glutaraldehyde (GLU) was developed to show a robust and efficient detection platform (Figure 1). This study was further validated using a small subset of clinical samples.

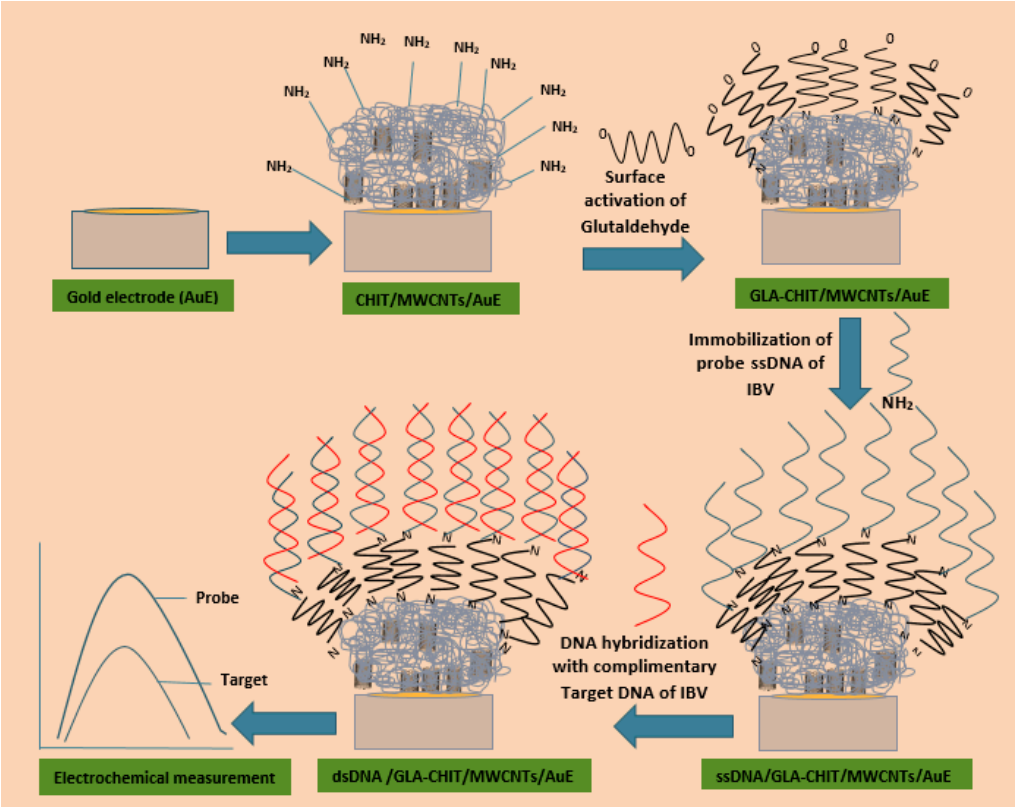

Figure 1. Schematic representation of the DNA modification process showing the attachment of probe DNA to the surface of chitosan and multi-walled carbon nanotubes (CS-MWNTs) using glutaraldehyde (GTD).

2. Materials and Methods

2.1. Materials and Chemicals

The electrochemical experiments were conducted using a μautolab potentiostat/galvanostat system (model PGSTAT) with NOVA Autolab 1.8 software. Cyclic voltammetry (CV) and differential pulse voltammetry measurements (DPV) were performed using the potentiostat, and the presence of target molecules was assessed based on the current response observed in the voltammograms. A Metrohm gold disk electrode (3 mm) was used as a substrate for the covalent immobilization of the oligonucleotide probe. The pH measurements were carried out using a Metrohm pH meter (model 691) connected to a glass electrode during the experiments. The C1000™ Thermal Cycler (Bio-Rad Laboratories, Inc., Hercules, CA, USA) was used to amplify DNA segments via the polymerase chain reaction (PCR).

The chemicals for the buffer preparation (potassium hydrogen phosphate (K_2HPO_4), potassium dihydrogen phosphate (KH_2PO_4), sodium citrate dihydrate ($C_6H_9Na_3O_9$), and sodium chloride (NaCl) were purchased from Systerm Chemicals, Malaysia, and EDTA (ethylenediaminetetraacetic acid) ($C_{10}H_{16}N_2O_8$) was purchased from Sigma-Aldrich, USA. Redox indicator chemicals, potassium hexacyanoferrate (III) and potassium ferrocyanide (II) trihydrate, were sourced from Nacalai Tesque (Japan). Methylene blue and iron (III) chloride were obtained from Systerm Chemicals, Selangor, Malaysia, while Prussian blue (PB) was purchased from Sigma-Aldrich, USA. The PCR-amplified real IBV samples (allantoic fluid from chicken eggs) and samples of different viruses and bacteria were collected from the Veterinary Department of Sabah, Malaysia. The oligonucleotides tested in this study (Table 1) were synthesized by First BASE Laboratories Sdn. Bhd, Selangor, Malaysia. A 50 mM Tris-HCl buffer solution containing 20 mM NaCl (pH 7.0) was prepared using reagents from Sigma-Aldrich, USA, as a supporting electrolyte and washing buffer for

cyclic voltammetry measurements. The hybridization buffer was prepared using a 0.3 M NaCl and 30 mM sodium citrate buffer solution (2× SSC buffer) at pH 6.0.

2.2. Preparation of Chitosan-Modified MWCNTs Solution

MWCNTs were functionalized with carboxylic groups (COOH) using a 3:1 ratio of sulfuric and nitric acid solutions. The mixture was stirred for 3 h, covered with aluminum foil, and homogenized. The resulting f-MWCNTs are denser than pure water and can be used for sensing applications. A 1% acetic acid solution was prepared with 1% CS powder, and 0.08 g f-MWCNTs were added. The process was repeated with a higher concentration of chitosan, resulting in a highly dispersed colloidal suspension in which bonds formed between the amino (NH_2) group of CS and the carboxyl (COOH) group of MWCNTs, as previously described by Ghica et al. [29].

Table 1. Nucleotide sequence of primer and probe for the detection of IBV.

Primer	Sequences (5′-3′)	References
Probe sequence	5′-NH2-CACCACCAGAACCTGTCACCTC-3′	[27]
Target sequence	5′-GAGGTGACAGGTTCTGGTGGTG-3′	(This study)
One-base mismatch	5′-GAGGTGACACGTTCTGGTGGTG-3′	(This study)
Three-base mismatch	5′-GAGGTCACAGATTCTGGCGGTG-3′	(This study)
Non-complementary	5′-GCCATGTTGTCACTGTCTATT-3′	(This study)
Target DNA of ND	5′-GTGCAGGCACCCCRAGTGCT-3′	[28]
Target DNA of MG	5′-CGCAATTTGGTCCTAATCCCCAACA-3′	[30]
Target DNA of ILT	5′-CTAACCCGTTCGCCGCACTCG-3′	[27]
Target DNA of AIV	5′-TCAGGCCCCCTCAAAGCCGA-3′	[31]

ND, Newcastle disease; MG, *Mycoplasma gallisepticum*; ILT, infectious laryngotracheitis; AIV, avian influenza virus.

2.3. Preparation of DNA Oligonucleotides

DNA oligonucleotide stock (100 µM) solutions were prepared in a TE buffer solution containing 10 mM Tris-HCl and 1 mM EDTA (ethylenediaminetetraacetic acid) (pH 8.0) and kept frozen. Additional dilute solutions of the oligomers were prepared in a buffer containing 50 mM Tris-HCl and 20 mM NaCl at pH 7.0. For biosensor work, a 10 µM working solution was prepared from a 100 µM stock solution. From this working solution, the volume study for immobilization was conducted using a range of 25 µL (0.25 µM), and for hybridization, a range of 20 µL (0.2 µM) was used after a period of optimization. For long-term stability, the stock solutions were stored at −20 °C or lower, as required, and the appropriate dilutions were prepared immediately before use.

2.4. Construction of DNA Biosensor

Pre-treatment of the bare gold electrode (AuE) was performed following the method described by Siddiquee et al. [32]. Firstly, AuE was polished with a 0.3–0.5 µm alumina slurry for 2 min. The electrode was then gently rinsed with distilled water and further cleaned using an ultrasonic cleaner for 2 min. After cleaning, the electrode was dried using nitrogen gas. A 5 µL volume of the CS-modified MWCNTs solution was deposited onto the surface of the AuE and left to dry for 2 h. Then, the electrode, along with the counter electrode (platinum) and reference electrode (silver chloride), was immersed in a 50 mM Tris-HCl solution. A three-electrode cell configuration was employed to measure the current, representing the flow of charge through the electrolyte solution. To create a CS/MWCNTs/AuE nanocomposite film, another 5 µL solution of the prepared CS/MWCNTs was applied to the AuE surface as part of the pre-treatment and allowed to dry at room temperature. Subsequently, the electrode was washed with distilled water and immersed in a 1% glutaraldehyde solution for 2 h, resulting in a modified electrode referred to as GLU/CS/MWCNTs/AuE.

2.5. Physical Characterization

The physical characterization of the synthesized nanomaterials was observed under scanning electron microscopy (SEM) (Hitachi S-3400N Hitachi High-Technologies Corporation, Tokyo, Japan) and transmission electron microscopy (TEM) (FEI Tecni G2 Spirit BioTWIN, Thermo Fisher Scientific, Hillsboro, OR, USA). Briefly, 5 µL of synthesized nanomaterials was dissolved in chitosan. The pH of the mixture was measured using a pH meter (OAKTON PH 700 Benchtop pH Meter, Cole-Parmer, Vernon Hills, IL, USA).

2.6. Optimization of Immobilization and Hybridization

A glutaraldehyde-modified electrode (GLU/CS/MWCNTs/AuE) was developed for the detection of IBV. DNA immobilization and hybridization were conducted using the dipping method. The immobilization process involved immersing the electrode in an immobilization buffer (50 mM Tris-HCl + 20 mM NaCl, pH 7.0) containing 0.25 µM of amine-modified single-stranded DNA (ssDNA). The probe immobilization parameters were optimized based on time and temperature.

For hybridization, the ssDNA-GLU/CS/MWCNTs/AuE electrode was immersed in 1 mL of hybridization buffer (2× SSC buffer, pH 6.0) containing 0.2 µM of target DNA. Hybridization tests were conducted using the ssDNA-GLU/CS/MWCNTs/AuE with complementary, non-complementary, mismatched, and non-IBV oligonucleotide sequences. The electrode surface was thoroughly washed after each step to ensure accuracy and remove unbound molecules.

2.7. Electrochemical Analysis

Methylene blue (MB) was adsorbed onto the probe-modified AuE electrode by immersing it into a stirred solution of 50 mM Tris-HCl + 20 mM NaCl, pH 7, for 2 min without applying any potential to the electrode. After MB attachment, the electrode was rinsed with 50 mM Tris-HCl + 20 mM NaCl at pH 7.0. The reduction signal of MB was measured using DPV in the range of 0.9 V to −0.1 V and CV in the range of 0.0 V to 1.7 V, with a modulation amplitude of 50 mV and a scan rate of 150 mV/s. The same protocols were carried out for the probe-modified AuE electrode after hybridization with target or non-complementary sequences. All experiments were conducted in an electrochemical cell at room temperature condition of 21 ± 2 °C unless specified otherwise. Data analysis was performed using a potentiostat/galvanostat for the electrochemical apparatus.

2.8. IBV Screening by RT-PCR

All positive samples were taken from IBV-infected commercial poultry flocks inTuaran, Sabah, Malaysia [29], and were used to develop and validate this sensor-based diagnostic method. Briefly, three pooled organ swab samples (trachea, kidneys, and lungs) were collected using Citoswab with 3 mL of VTM medium from 10 different flocks (n = 5). Sampling was conducted based on gross pathological findings suggestive of IBV infection, identified during post-mortem examination and previously confirmed using PCR [29]. The IBV RNA was extracted from allantoic fluid from incubated chicken eggs using the EasyPure® Viral DNA/RNA Kit (China). The extracted RNA was then stored at −70 °C until further use. Reverse transcription was performed using TransScript® II All-in-One First-Strand cDNA Synthesis SuperMix (China) for qPCR. All IBV isolates were tested using RT-PCR to detect conserved sequences of the 5′-UTR regions of IBV. Amplification was performed using the following forward 5′-GCTTTTGAGCCTTAGGTT-3 and reverse 5′-GCCATGTTGTCACTGTCTATTG-3 primers [23]. The thermal cycling program for amplification began with an initial denaturation step at 95 °C for 2 min, followed by 34 cycles comprising 45 s each at 94 °C, 55 °C, and 72 °C. Subsequently, a final extension of

5 min at 72 °C was performed, followed by cooling at 4 °C, and gel electrophoresis was conducted. To assess the specificity of the IBV primers, RT-PCR targeting the 5′UTR region of IBV was conducted on samples of various non-IBV pathogens, such as avian influenza virus, Newcastle disease virus, *Avibacterium paragallinarum*, infectious laryngotracheitis virus, *Mycoplasma gallisepticum*, and *Escherichia coli*, as outlined previously by Bhuiyan et al. [33].

2.9. Hybridization Experiment Using cDNA and PCR Positive Samples

The electrochemical DNA biosensor was evaluated by hybridizing the probe-modified electrode with cDNA synthesized from RNA extracted from IBV-infected clinical samples. Approximately 20 µL of cDNA was used for voltametric measurements. The process involved pre-treatment, immobilization of the probe, and hybridization with the DNA fragments obtained from PCR amplification onto the gold electrode surface. To obtain ssDNA, the diluted sample was denatured by heating in a water bath at 95 °C for 5 min and then cooled in an ice bath for 2 min. Control experiments were conducted with a positive real sample containing a PCR product with the complementary target sequence, a negative real sample without the target sequences, and the IBV probes with a PCR blank solution containing primers and polymerase but no amplified target DNA. The studies were performed in triplicate (n = 3) to ensure reproducibility, and the coefficient of variation (CV) for each of the three samples was determined. Table 2 shows the optimization parameters used for IBD detection.

Table 2. Optimized parameters were tested for the construction of DNA biosensor to detect IBV.

Parameters	Variation
Buffer solution	Acetate, Phosphate, Tris-HCl, Ammonium, Citrate
Redox indicator	MB, PB, and K_3 [Fe(CN)$_6$]
Scan rate/mVs^{-1}	50, 100, 150, 200, 250, 300
pH	6.0, 6.5, 7.0, 7.5, 80, 8.5
Accumulation time/sec	5, 10, 15, 20, 25
Probe volume/µL	5, 10, 15, 20, 25
Target volume/µL	5, 10, 15, 20, 25
Immobilization temperature/°C	30, 40, 50, 60
Immobilization time/min	15, 30, 45, 60
hybridization temperature/°C	30, 40, 50, 60
hybridization time/min	15, 30, 45, 60
Hybridization specificity (comparative study)	ND, MG, AIV, ILT

3. Results

3.1. Electrochemical Characteristics of the Modified AuE

The AuE surface was modified with NH_2 DNA, and detection was conducted using cyclic voltammetry (CV) by measuring the reduction signal of MB-labeled oligonucleotides. The electrochemical cell employed a hybridization buffer at pH 6.0, with a sensor potential range from +0.0 V to 1.7 V applied to the AuE. Bhuiyan et al. [34] previously optimized parameters to enhance the binding capacity of IBV target DNA using an unmodified AuE, showing a peak current of 0.076 mA at the binding point. In the current study, the focus shifts to employing a modified AuE with different nanomaterials to increase hybridization efficiency. When a CS film was applied, it affected the electrode's potential, shifting it towards the formal potential and significantly increasing peak-to-peak changes to 2.71 mA. This indicates an alteration in the electron transfer kinetics at the electrode surface. The findings suggest that CS slows the electron transfer kinetics of MB, likely due

to its low electrical conductivity. However, incorporating conductive materials, such as gold nanoparticles with redox-active components, into the CS layer could counteract its insulating properties and potentially enhance the current further.

To enhance the electrical signal, functionalized MWCNTs were incorporated into the CS film, creating a CS/MWNTs/AuE electrode, which showed a peak current of 3.29 mA. Further modification with 1% glutaraldehyde and 5 µM of the redox solution MB resulted in slightly lower peak currents of 3.05 mA due to the increased film thickness, which inhibited electron transfer kinetics. The modified ssDNA-GLU/CS/MWCNTs/AuE electrode was employed to optimize the parameters of the developed biosensor. The results showed that the redox peak currents and peak separation potential were higher for the modified AuE compared to the bare AuE used during sequential modifications. Figure 2C,D show the CS/MWCNT/AuE nanocomposite film as examined under a scanning electron microscope (SEM) and a transmission electron microscope (TEM), respectively. Figure 2C reveals the presence of microscopic holes, indicating the improved performance of the CS/MWCNT/AuE combination as a sensor. The porous membrane in Figure 2C results from the addition of CS to the MWCNT, described as well-dispersed pipe bundles when magnified at 50 nm with the TEM (Figure 2D).

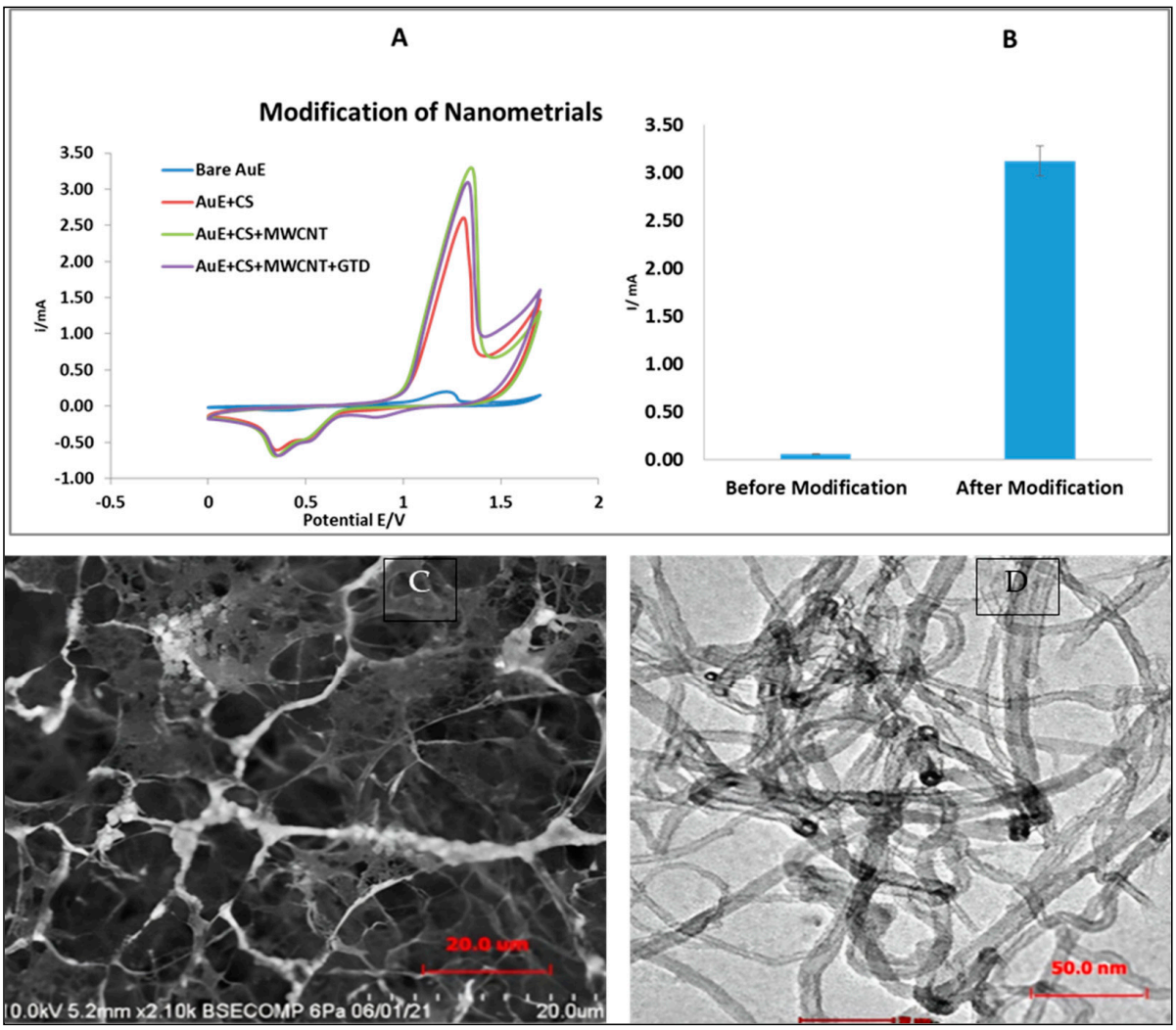

Figure 2. Cyclic voltammetry (CV) (0.0 to 1.70 V) recorded on a gold electrode (AuE) with different modifications of the AuE surface (**A**) and before and after modification (**B**), supported by MB redox (5 mM) at a scan rate of 0.20 mV·s^{-1} vs. Ag | AgCl (*I*—current, *E*—potential) (n = 3). (**C**) SEM under 20 nm magnification, (**D**) TEM under 50 nm magnification.

3.2. Effect of Time and Temperature (Immobilization and Hybridization)

The effectiveness of DNA immobilization and hybridization was influenced by both the time and temperature. To optimize the immobilization of ssDNA onto the GTD/CS-MWCNTs/AuE, 25 µL of ssDNA (0.25 µM) was studied under varying conditions: durations of 15, 30, 45, and 60 min and temperatures of 30 °C, 40 °C, 50 °C, and 60 °C. As shown in Figure 3A, the optimal immobilization activity was observed under conditions that yielded an increased CV peak current, which gradually decreased with longer durations and higher temperatures.

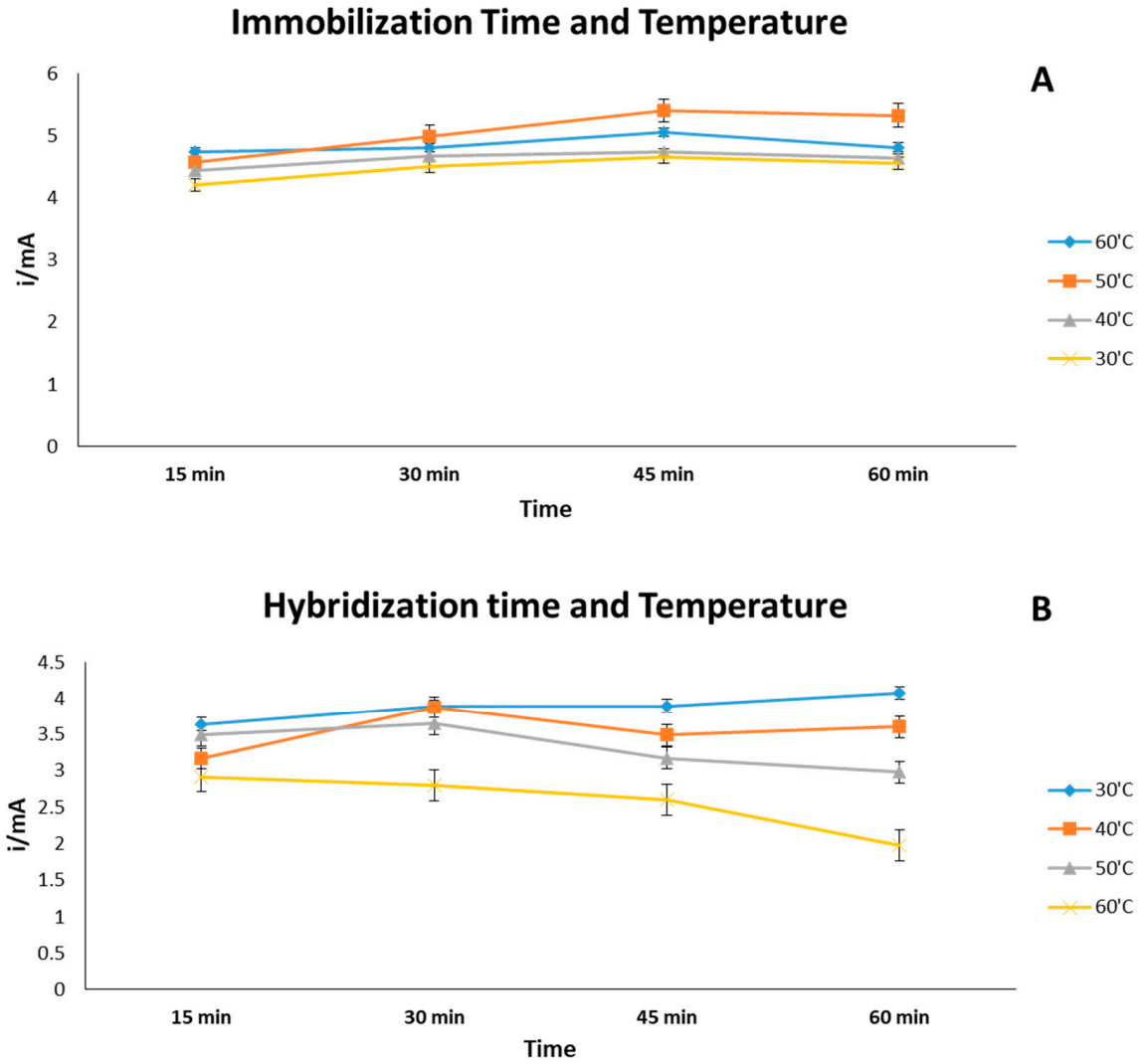

Figure 3. (**A**) Effect of immobilization and (**B**) hybridization time and temperature on modified AuE supported by MB (5 mM) using cyclic voltammograms (CV) supported by MB redox (5 mM) at a scan rate of 0.20 mV·s^{-1} vs. Ag | AgCl (*I*—*current*, *E*—*potential*) (n = 3).

Based on the current signal, the optimal conditions for ssDNA immobilization were determined to be 45 min at 50 °C, which were used for further biosensor development. Subsequently, the modified ssDNA-GLU/CS/MWCNTs/AuEs were hybridized with 20 µL of an optimized target DNA solution (0.2 µM) at different temperatures (30 °C, 40 °C, 50 °C, and 60 °C) and durations (15, 30, 45, and 60 min). As shown in Figure 3B, the DNA hybridization increased between 30 and 60 °C and within 15–60 min but gradually decreased beyond 60 min and at temperatures above 50 °C. Therefore, the optimal hybridization conditions were set at 30 °C for 60 min. The efficiency and stability of hybridization were evaluated by analyzing the interaction of MB with the DNA probe.

3.3. Quantitative Analysis of Target DNA and Sensitivity

In this study, DPV was used to assess the sensitivity and detection limit of the modified GLU/CS/MWCNTs/AuE biosensor. The results, shown in Figure 4A, illustrate the DPV response to different concentrations of the IBV target DNA sequence in a hybridization buffer (pH 6.0) containing 5 mM of the redox indicator MB. The data showed that the intensity of the DPV current peak for MB on the GLU/CS/MWCNTs/AuE gradually decreased as the concentration of target DNA increased.

A

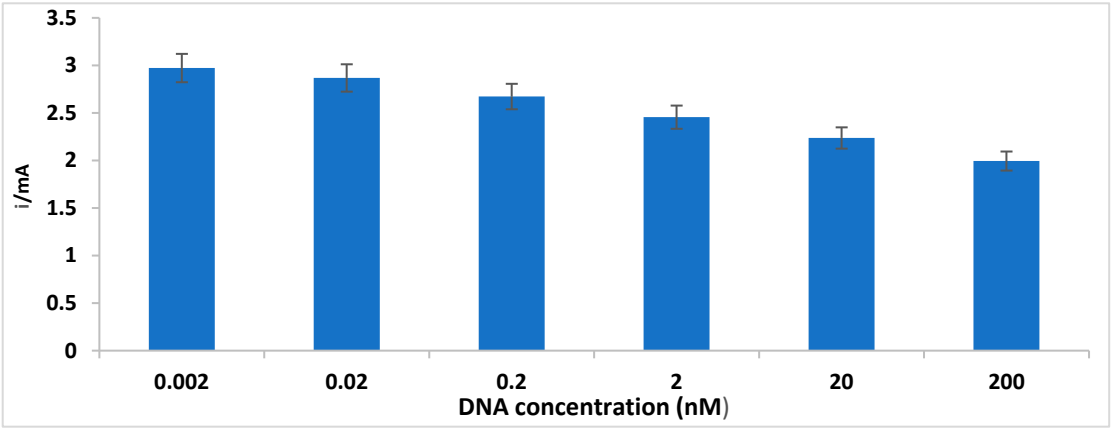

B

	LoD = 3σ/m
	σ = SD of blank solution, 0.017365
	m = slope of the calibration plot (y=mx + c), y = 0.2002x + 0.646
LoD	0.26
	LoD = 0.26 nM
	LoQ = 10σ/m
	σ = SD of blank solution, 0.017365
	m = slope of the calibration plot (y=mx + c), y = 0.2002x + 0.064
LoQ	0.79
	LoD = 0.79 nM

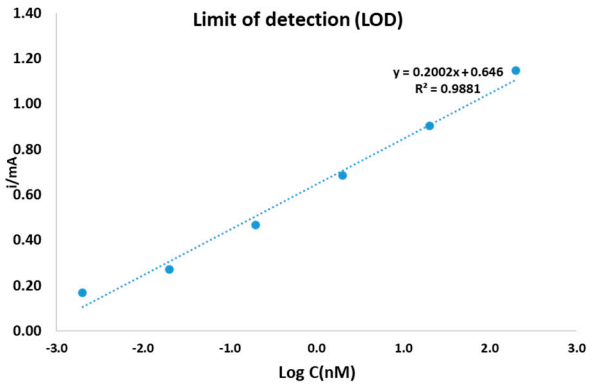

Figure 4. DPV analysis of different concentrations of target DNA: (**A**) bar chart and (**B**) linearity supported by MB redox (5 mM) at a scan rate of 0.20 mV·s^{-1} vs. Ag | AgCl (*I*—*current*, *E*—*potential*) (n = 3).

A calibration curve of the current signals (ΔI) was constructed using the 3 σ/*m* formula to calculate the limit of detection (LOD) and the 10 σ/m formula to determine the limit of quantification (LOQ), where σ is the standard deviation of the blank solution, and *m* is the slope of the linear curve). As shown in Figure 4B, at potential value of −0.1 V and 0.9 V, a linear regression equation (y = mx + c), y = 0.2002x + 0.646, with a correlation coefficient of R_2 = 0.98, was derived by plotting the logarithmic value of the reduced MB peak current against the logarithmic values of synthetic IBV target DNA concentrations, ranging from 0.2 µM to 0.002 nM. The LOD and LOQ for the proposed biosensor were calculated as 0.26 nM and 0.79 nM, respectively.

3.4. Reproducibility, Repeatability, and Storage of the Biosensor

Reproducibility, repeatability, and storage are essential parameters for evaluating the performance of the developed DNA biosensor. Repeatability and reproducibility tests were conducted by analyzing the variations in the oxidation peak current during hybridization

across five different electrodes. The results showed good reproducibility, with RSD values of 3.19% and 5.01% (n = 5), indicating high reproducibility and repeatability.

The stability of the modified electrode (ssDNA-GLU/CS/MWCNTs/AuE) was examined after storage and hybridization with 0.2 µM target DNA for 7, 14, 21, and 28 days to evaluate the percentage of signal recovery. In this study, the modified electrode was stored at room temperature conditions of 20 ± 2 °C. As shown in Figure 5, the modified probe exhibited excellent stability when stored for 5 weeks, resulting in only a 5.5% decrease in the initial signal response.

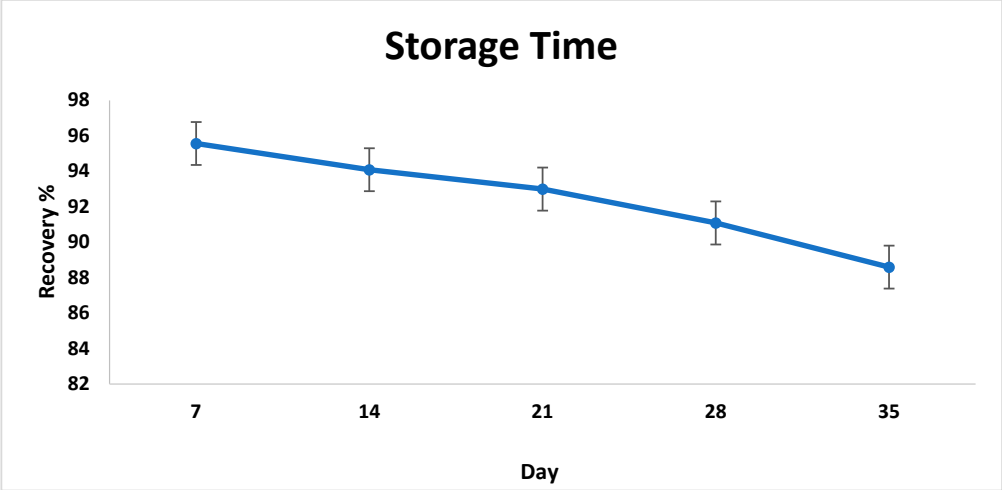

Figure 5. The recovery percentage of the sensor stability after storage of 7, 14, 21, 28, and 35 days of interval time of the MB reduction peak current using different hybridization effects supported by MB redox (5 mM) at a scan rate of 0.20 mV·s^{-1} vs. Ag | AgCl (*I*—*current*, *E*—*potential*) (n = 3).

3.5. Validation of Developed Biosensor Using Field Samples

The developed DNA-based biosensor with a modified IBV probe was validated using cDNA and PCR-amplified IBV samples under optimal parameters. Figure 6A shows that the CV response of three positive IBV samples exhibited the lowest current signal compared to other non-IBV samples relative to the synthetic target DNA signal. In three subsequent experiments, the proposed biosensor (ssDNA/GTD/CS/MWCNTs/AuE) showed the highest recovery in detecting IBV in positive real samples. The developed biosensor showed average MB signals of 4.19 mA, 3.99 mA, and 3.83 mA for the three positive samples, with RSD values of 4.66%, 1.29%, and 2.32%, respectively. In addition, recovery values of 95.41%, 99.38%, and 99.55% were obtained for these samples, as shown in Table 3.

Table 3. Recovery and RSD value of cDNA and PCR in IBV positive real samples (n = 3).

+Real IBV Sample	cDNA		PCR
	RSD Value	Recovery %	RSD Value
Sample 1	4.66	95.41	4.65
Sample 2	1.29	99.38	3.27
Sample 3	2.32	99.55	7.05

Figure 6B shows the hybridization evaluation between the modified IBV probe and the target DNA sequence from the positive PCR samples. The results show a significant decrease in MB signals in positive real samples 1, 2, and 3, which contained the specific target sequence, compared to the signals from the synthetic target DNA. Conversely, negative real samples treated with the modified probe showed no hybridization activity, resulting in a significant difference between the MB signal and the probe signal. The signal detected in the

PCR blank solution showed a slight increase in the MB signal, which was still lower than the probe signal. This can be attributed to the interaction between MB and free guanine bases in the single-stranded primers present in the PCR blank solution. After hybridization, the average MB signals of the three positive samples were 3.91 mA, 3.98 mA, and 4.01 mA, respectively. The relative standard deviation (RSD) of the MB signal for hybridization was 4.65%, 3.27%, and 7.05%, respectively. These RSD values, all below 10%, indicated good precision and reproducibility (see Table 3). Prior to analyzing the real samples, PCR with universal primers was performed to amplify three PCR products, resulting in fragments of approximately 143 base pairs (bp) as confirmed by gel electrophoresis (Figure 6C). The coefficient of variation (CV) values of the samples ranged from 5.0% to 8.34%, indicating consistency and minimal variability, supporting further research. The experiments were conducted in triplicate (n = 3) to ensure reproducibility, and the coefficient of variation (CV) for each of the three samples was calculated.

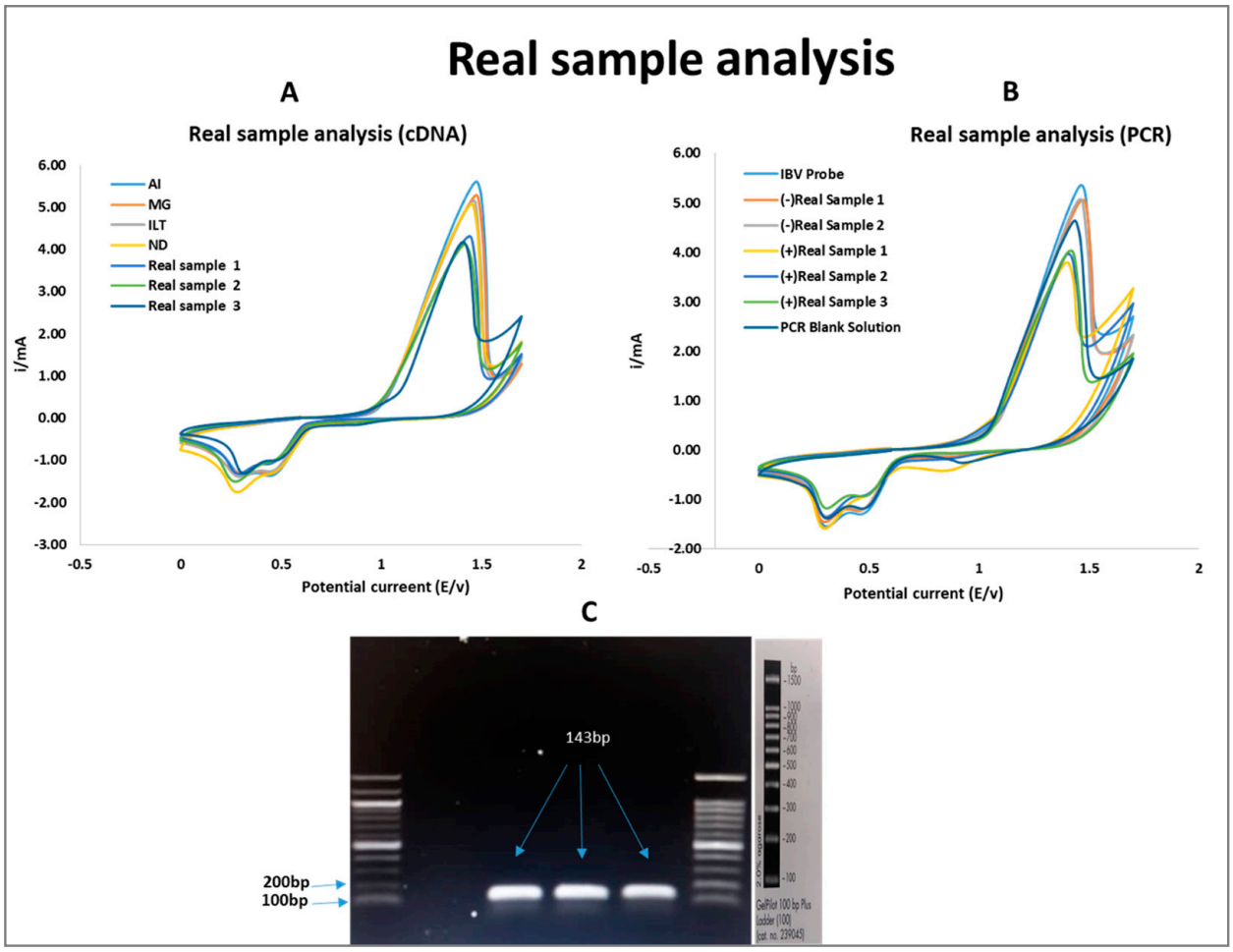

Figure 6. The electrochemical analysis (CV) of the MB reduction peak current for real sample study using probe-modified biosensor against target IBV DNA at a scan rate of 0.2 V/s vs. Ag|AgCl (*I*—*current*, *E*—*potential*) (n = 3). (**A**) Extracted cDNA from IBV-positive samples was tested against non-IBV target DNA. (**B**) PCR-amplified IBV-positive samples and negative controls, including a PCR blank. (**C**) Agarose gel electrophoresis of the PCR-amplified IBV 5-UTR region, in which a 143 bp positive band was detected in three farm isolate samples, confirming the presence of IBV.

This study initially required extensive adjustment of parameters such as pH, scan rate, and storage conditions; however, once these were optimized, the experimental procedure became much faster and more effective. As DNA biosensors do not require gel extraction, they can often provide results in less than 80–100 min, making them faster than PCR. First,

the infected sample must be prepared, which takes about 20 min and involves extracting the DNA from the sample. A specific DNA probe is then fixed to a gold-modified electrode for around 40 min. This is followed by hybridization, which takes about 20 min, during which the IBV target DNA binds to the immobilized probe. Finally, it takes about 5 min to examine the quantifiable signal by electrochemical measurement with CV and DPV as well as MB as a redox indicator to identify hybridization events. The entire biosensor procedure takes approximately 80 min.

Table 4. Previous studies on gammacoronaviruses (γCoVs) detection using other biosensor techniques.

Type of Sensor	Biosensing Concept	Detection Limit	Reference
Electrochemical biosensor (5′-UTR region of the IBV genome)	Modification with nanoparticles (GLU/CS/MWCNTs/AuE)	2.6×10^{-10} mol L^{-1} (0.26 nM)	This study
Electrochemical biosensor (Spike-S gene)	Modification with nanoparticles and functionalized AuNPs (gold nanoparticles)	2.96×10^{-16} mol L^{-1}	[35]
Fluorescent immunosensor	Ab (antibody)-functionalized MoS2 (molybdenum disulfide)	460 EID50/mL	[36]
Immunosensor	ICS (Inorganic Carbon Sphere) with Au NP-conjugated antibodies	104.4 EID50	[37]

4. Discussion

In this study, a DNA biosensor was developed for the direct electrochemical detection of any IBV strain by targeting the 5′UTR region of the IBV genome. The successful development of an electrochemical DNA biosensor relies on selecting an appropriate immobilization technique, molecular recognition method, and chemical reaction to construct the surface architecture [38]. Optimization results show that the modification of AuE significantly enhances the sensing capacity of the developed biosensor and exhibits excellent electron conductivity. The findings align with those of Wang et al. [39], who demonstrated that nanomaterial modification of electrodes improves signal processing by grafting materials onto the electrode surface and generating visible signals with different modification layers onto the AuE surface. The peak currents provide quantitative information about the analyte concentration and detection range, while the peak separation potential ensures specificity, reliability, and the ability to discriminate between different redox reactions. SEM and TEM analyses of the CS/MWCNT/AuE nanocomposite film show the presence of microscopic holes, indicating enhanced sensor performance. The porous membrane formed from the addition of CS to MWCNTs is well dispersed, as observed in TEM images. Zhao et al. [40] corroborated these findings, describing the porous membrane in Figure 2C as a result of CS addition to the MWCNT, appearing as well-dispersed pipe bundles when magnified at 50 nm (Figure 2D). Shalauddin et al. [41] reported that functionalizing MWCNTs into MWCNTs-COOH using sulfuric and nitric acids enables the determination of specific target elements. The presence of O-H and N-H bonds in the CS/MWCNTs contributes to higher current signals, further supporting the biosensor's effectiveness.

The peak currents provide quantitative analyte information, while peak separation potential ensures specificity and the ability to differentiate redox reactions. Studies by Markegard et al. [42] indicated that DNA hybridization effectiveness increases with time until it reaches a steady state. This study found that the hybridization temperature and time affect the peak reduction current of MB, with optimal conditions being 30 °C and 60 min, respectively. Temperatures above 50 °C risk DNA denaturation, reducing the detection signal. Similar studies by Nimse et al. [43] and Benvidi et al. [44] emphasize the importance

of precise hybridization temperature for efficient DNA binding, supporting findings that recommend an optimal temperature between 30 °C and 35 °C.

In addition, the reproducibility and repeatability of several assays with equivalent RSD results ranging from 2 to 6% suggest that the constructed biosensor has good reproducibility for the detection of IBV target DNA [45–47]. According to Nordin et al. [38], the modified probe was very stable, with more than 80–90% of the original signal still detectable after 2–6 months. The storage results suggest that the strong binding capacity between the modified electrode CS/MWCNTs and glutaraldehyde contributes to the long-lasting stability of AuE and acts as an electron transfer mediator in the proposed biosensor [48]. Although our results are still below specification, optimizing the hydrogel coating for long-term biosensor storage is a potential solution that will be explored in future studies as resources permit.

The positive samples were tested with a specific IBV primer to differentiate IBV from non-IBV pathogens, such as Newcastle disease virus, infectious laryngotracheitis virus, avian influenza virus, infectious bursal disease virus, and *Mycoplasma gallisepticum*, and to validate the specificity of the IBV probe used in our DNA biosensor study [33]. The developed DNA-based biosensor with a modified IBV probe was tested with different positive IBV samples under optimal parameters. The positive samples were confirmed using PCR with universal primers, producing fragments of approximately 143 base pairs (bp), as verified by gel electrophoresis, which indicated the presence of IBV target DNA in the samples. In addition, the extracted cDNA was used to prepare the biosensor for IBV identification, which allowed for comparison with different types of non-IBV samples and evaluation of analytical performance. It was found that the proposed biosensor (ssDNA/GLU/CS/MWCNTs/AuE) showed different signal responses after hybridization with different types of genomic nucleic acids extracted from the Newcastle disease virus, infectious laryngotracheitis virus, avian influenza virus, infectious bursal disease virus, and *Mycoplasma gallisepticum*.

Several studies have focused on synthetic oligonucleotides, highlighting their ability to detect hybridization through current signals. Although only a limited number of studies have been discussed, the reliable measurements that can be obtained from hybridization events with cDNA and PCR-amplified products from real infected samples are of clinical interest [45,49]. Analysis of field samples revealed that MB has a stronger binding affinity to the ssDNA surface than to dsDNA. [50–53]. Consistent results were obtained for the reproducible values, which showed similar trends in the coefficient of variation (CV). When the real IBV samples (cDNA and PCR amplicon) were exposed to the modified probe GLU/CS/MWCNTs/AuE, the peak current of CV showed a decrease and averaged 4.25 mA–3.99 mA, with a relative standard deviation (RSD) of less than 5–10%. This range is generally considered to be good and aligns with many previous studies [54,55]. In addition, our results showed a satisfactory recovery correlation between 94.51% and 99.55% when the biosensor was used to identify the modified probe DNA sequences recovered from both cDNA and real PCR samples of IBV. These results are consistent with previous reports on DNA biosensor studies [56,57]. The accuracy and portability of this biosensor make it particularly useful for chicken farms where rapid disease management depends on detection and intervention. At the point of care, the proposed biosensor can provide near-instant detection, unlike conventional techniques that often experience delays due to sample transportation and laboratory processing.

For IBV or similar viruses, the LOD of 2.6 nM is comparable to or better than the sensitivity of several reported electrochemical biosensors, which typically range from 1 nM to 10 nM [58]. This is in contrast to other biosensor-based techniques, such as graphene nanoparticle-based biosensors. According to some studies, a graphene oxide-

based dopamine biosensor has a detection limit of 3.2 nM [59]. In contrast, fluorescence-based techniques generally offer lower LOD values than electrochemical sensors. However, they may not be as stable or specific in complex biological samples. The combination of MWNTs, chitosan, and glutaraldehyde improves the biosensor by ensuring stable attachment of the probe and preventing signal loss. This innovation overcomes challenges such as low sensitivity, high detection limits, and instability common to conventional methods. It provides a fast, sensitive, and cost-effective solution for IBV diagnostics and offers practical and scalable benefits, especially in resource-constrained environments.

The identification of avian gammacoronaviruses (γCoVs) using different biosensor approaches has already been investigated, as shown in Table 4. According to previous research, only one study on gammacoronavirus used an electrochemical DNA biosensor, while the other two used an immunobiosensor. A label-free electrochemical approach to detect the spike (S) gene of the H120 strain was described in a previous work by Yang et al. [35], but the detection limit was slightly lower than our results. The primary goal of the previous study was to establish a target DNA sequence (S gene) that can recognize the H120 RNA when it forms a DNA-RNA hybridized double-stranded structure. As everyone knows, RNA is very unstable at normal temperatures and can easily degrade in the environment unless it is stored at -70 °C. In addition, the S gene in the genome is highly mutated, which requires a constant change in primer selection. Instead of the S gene, we used the universal 5′-UTR region of the IBV genome for our study, which has a relatively low mutation rate and can detect all types of IBV strains. These results emphasize the potential of developing biosensor-based techniques for the diagnosis of viral diseases in poultry.

When comparing the sensitivity, specificity, and reproducibility of the TaqMan probe-based qPCR, or SYBR-Green-based qPCR or the ELISA method for the detection of viruses with the electrochemical DNA biosensor for IBV detection, both methods show higher performance but with different advantages and limitations. With an impressively low limit of detection (LOD) of 2.6 nM in this study, the DNA biosensor demonstrated an exceptional detection range of 2.0×10^{-12} to 2.0×10^{-5} mol/L. This performance is significantly better compared to ELISA methods, which typically exhibit higher LOD values, often exceeding 1 ng/m. This substantial improvement in sensitivity ensures that the biosensor can detect IBV at much lower concentrations, enabling earlier diagnosis and intervention during an outbreak. TaqMan-based qPCR offers high sensitivity (10–100 copies/µL) and specificity for the detection of viruses, especially in multiple infections [60,61], whereas the electrochemical DNA biosensor, despite its comparable sensitivity for IBV (2.6 nM), is limited to the detection of single pathogens due to single probe selection. This limitation restricts the current DNA biosensor's ability to effectively detect emerging IBV variants (GI, GII, GIII, GIV). The concept utilizes multiple probes from the genomic DNA of local IBV strains linked to electrode arrays, but further research is needed to improve the specificity of the biosensor. As far as reproducibility is concerned, both methods have been thoroughly validated in their respective studies. While the DNA biosensor also shows consistent results when analyzing IBV in real samples from farms, it can be difficult to maintain reproducibility with different pathogen strains or in environments with varying sample quality. Compared to conventional RT-PCR assays, which cost USD 20 to USD 50 per sample, the DNA biosensor is far less expensive and offers better sensitivity and specificity, with an estimated cost of USD 1 to USD 5 per sample, assuming the nanomaterial is used efficiently. One of the limitations of these biosensors is that they can only detect once the DNA has been extracted from the infected sample, and they are then used in equipment that is difficult for farmers to operate. Therefore, where possible, chicken blood should be tested directly with a device whose sensitivity needs to be improved through further

research and biosensor development. Advanced ELISA tests, DNA amplification methods, and next-generation sequencing analysis could further improve biosensor technology. This study acknowledges the limitation of a small sample (n = 3), which compromises wider applicability. Future work will involve testing a larger and more diverse sample to increase reliability and credibility. The optimization parameters identified in this study will contribute to the modification of a portable device that enables faster diagnosis of chicken diseases and facilitates prompt preventive measures, thereby reducing losses for farmers.

5. Conclusions

This study successfully optimized the parameters for a modified AuE in the development of a biosensor for the universal detection of all IBV strains. The incorporation of GLU as a linker facilitated the covalent immobilization of probe sequences on the AuE surface, in conjunction with CS and MWNTs, enhancing the sensor's performance. The experimental results showed the biosensor's ability to clearly differentiate complementary, non-complementary, and mismatched oligonucleotides based on MB-DNA interactions, yielding significantly improved hybridization signals. Under optimized conditions, the electrochemical DNA biosensor achieved an LOD as low as 2.69 nM, with a linear detection range from 2.0×10^{-12} to 2.0×10^{-5} mol L^{-1}. The developed biosensor effectively detected IBV in a small subset of clinical samples and successfully discriminated between IBV and non-IBV organisms, highlighting its high specificity under controlled conditions. However, as a proof-of-concept study, this method requires further validation using a large number of clinical samples before it can be implemented for regular monitoring of IVB in farms. Further research should focus on integrating multiple probe sequences targeting different genomic regions of IBV and developing a multi-electrode platform to further enhance detection accuracy and diagnostic capability.

Author Contributions: Conceptualization, M.S.A.B., G.R. (Gilbert Ringgit) and Z.A.; investigation, S.S. (Suryani Saallah); resources, A.M.S.A.B.; writing—original draft preparation, M.S.A.B.; writing—review and editing, S.S. (Subir Sarkar), Z.A. and S.M.S.; supervision, S.S. (Shafiquzzaman Siddiquee), Z.A. and S.M.S. All authors have read and agreed to the published version of the manuscript.

Funding: This research was funded by the Research Grant (UMSgreat) Scheme (GUG108-1/2017). Subir Sarker is the recipient of an Australian Research Council Discovery Early Career Researcher Award (grant number DE200100367) funded by the Australian Government.

Institutional Review Board Statement: This study was conducted with the approval of the institutional animal ethics committee (Veterinary ethics, DVS (MDVKK) 600-5/18) on 23 May 2018. The guidelines for the Care and Use of Animals set by the Sabah Department of Veterinary Services, Sabah, Malaysia, were followed.

Informed Consent Statement: Not applicable.

Data Availability Statement: The original contributions presented in this study are included in the article. Further inquiries can be directed to the corresponding author.

Acknowledgments: The authors also like to thank all the scientists who have been directly or indirectly involved in the IBV study in this project.

Conflicts of Interest: The authors declare no conflicts of interest.

References

1. Serbessa, T.A.; Geleta, Y.G.; Terfa, I.O. Review on diseases and health management of poultry and swine. *Int. J. Avian Wildl. Biol.* **2023**, *7*, 27–38. [CrossRef]
2. Gržinić, G.; Piotrowicz-Cieślak, A.; Klimkowicz-Pawlas, A.; Górny, R.L.; Ławniczek-Wałczyk, A.; Piechowicz, L.; Wolska, L. Intensive poultry farming: A review of the impact on the environment and human health. *Sci. Total Environ.* **2023**, *858*, 160014. [CrossRef]
3. Lu, Y.; Zeng, Y.; Luo, H.; Qiao, B.; Meng, Q.; Dai, Z.; Ping, J. Molecular characteristic, evolution, and pathogenicity analysis of avian infectious bronchitis virus isolates associated with QX type in China. *Poult. Sci.* **2024**, *103*, 104256. [CrossRef] [PubMed]
4. Valastro, V.; Holmes, E.C.; Britton, P.; Fusaro, A.; Jackwood, M.W.; Cattoli, G.; Monne, I. S1 gene-based phylogeny of infectious bronchitis virus: An attempt to harmonize virus classification. *Infect. Genet. Evol.* **2016**, *39*, 349–364. [CrossRef]
5. Miranda, C.; Silva, V.; Igrejas, G.; Poeta, P. Genomic evolution of the human and animal coronavirus diseases. *Mol. Biol. Rep.* **2021**, *48*, 6645–6653. [CrossRef]
6. Cui, J.; Li, F.; Shi, Z.L. Origin and evolution of pathogenic coronaviruses. *Nat. Rev. Microbiol.* **2019**, *17*, 181–192. [CrossRef] [PubMed]
7. Kung, Y.A.; Lee, K.M.; Chiang, H.J.; Huang, S.Y.; Wu, C.J.; Shih, S.R. Molecular virology of SARS-CoV-2 and related coronaviruses. *Microbiol. Mol. Biol. Rev.* **2022**, *86*, e0002621. [CrossRef] [PubMed]
8. He, Y.; Xie, Z.; Dai, J.; Cao, Y.; Hou, J.; Zheng, Y.; Wei, P. Responses of the Toll-like receptor and melanoma differentiation-associated protein 5 signaling pathways to avian infectious bronchitis virus infection in chicks. *Virol. Sin.* **2016**, *31*, 57–68. [CrossRef]
9. Bhuiyan, M.S.A.; Amin, Z.; Bakar, A.M.S.A.; Saallah, S.; Yusuf, N.H.M.; Shaarani, S.M.; Siddiquee, S. Factor influences for diagnosis and vaccination of avian infectious bronchitis virus (Gammacoronavirus) in chickens. *Vet. Sci.* **2021**, *8*, 47. [CrossRef]
10. Najimudeen, S.M.; Abd-Elsalam, R.M.; Ranaweera, H.A.; Isham, I.M.; Hassan, M.S.; Farooq, M.; Abdul-Careem, M.F. Replication of infectious bronchitis virus (IBV) Delmarva (DMV)/1639 variant in primary and secondary lymphoid organs leads to immunosuppression in chickens. *Virology* **2023**, *587*, 109852. [CrossRef]
11. Bhuiyan, M.S.A.; Sarker, S.; Amin, Z.; Rodrigues, K.F.; Saallah, S.; Shaarani, S.M.; Siddiquee, S. Infectious Bronchitis Virus (Gammacoronavirus) in Poultry, Genomic Architecture, Post-Translational Modifications, and Structural Motifs. *Poultry* **2023**, *2*, 363–382. [CrossRef]
12. Vidic, J.; Vizzini, P.; Manzano, M.; Kavanaugh, D.; Ramarao, N.; Zivkovic, M.; Radonic, V.; Knezevic, N.; Giouroudi, I.; Gadjanski, I. Point-of-Need DNA Testing for Detection of Foodborne Pathogenic Bacteria. *Sensors* **2019**, *19*, 1100. [CrossRef] [PubMed]
13. Abu-Salah, K.M.; Zourob, M.M.; Mouffouk, F.; Alrokayan, S.A.; Alaamery, M.A.; Ansari, A.A. DNA-based nanobiosensors as an emerging platform for detection of disease. *Sensors* **2015**, *15*, 14539–14568. [CrossRef]
14. Ye, Q.; Lu, D.; Zhang, T.; Mao, J.; Shang, S. Recent advances and clinical application in point-of-care testing of SARS-CoV-2. *J. Med. Virol.* **2022**, *94*, 1866–1875. [CrossRef]
15. Arega, S.M.; Conraths, F.J.; Ameni, G. Prevalence of tuberculosis in pigs slaughtered at two abattoirs in Ethiopia and molecular characterization of Mycobacterium tuberculosisisolated from tuberculous-like lesions in pigs. *BMC Vet. Res.* **2013**, *9*, 97. [CrossRef]
16. Grabowska, I.; Stachyra, A.; Góra-Sochacka, A.; Sirko, A.; Olejniczak, A.B.; Leśnikowski, Z.J.; Radecka, H. DNA probe modified with 3-iron bis (dicarbollide) for electrochemical determination of DNA sequence of Avian Influenza Virus H5N1. *Biosens. Bioelectron.* **2014**, *51*, 170–176. [CrossRef]
17. Awad, F.; Forrester, A.; Baylis, M.; Lemiere, S.; Jones, R.; Ganapathy, K. Immune responses and interactions following simultaneous application of live Newcastle disease, infectious bronchitis and avian metapneumovirus vaccines in specific-pathogen-free chicks. *Res. J. Vet. Sci.* **2015**, *98*, 127–133. [CrossRef]
18. Ahmed, W.; Simpson, S.L.; Bertsch, P.M.; Bibby, K.; Bivins, A.; Blackall, L.L.; Shanks, O.C. Minimizing errors in RT-PCR detection and quantification of SARS-CoV-2 RNA for wastewater surveillance. *Sci. Total Environ.* **2022**, *805*, 149877. [CrossRef] [PubMed]
19. Robinson-McCarthy, L.R.; Mijalis, A.J.; Filsinger, G.T.; De Puig, H.; Donghia, N.M.; Schaus, T.E.; Church, G.M. Laboratory-generated DNA can cause anomalous pathogen diagnostic test results. *Microbiol. Spectr.* **2021**, *9*, e00313-21. [CrossRef]
20. Sheikhzadeh, E.; CHamsaz, M.; Turner, A.P.F.; Jager, E.W.H.; Beni, V. Label-free impedimetric biosensor for Salmonella Typhimurium detection based on poly [pyrrole-co-3-carboxyl-pyrrole] copolymer supported aptamer. *Biosens. Bioelectron.* **2016**, *80*, 194–200. [CrossRef]
21. Rashid, J.I.A.; Yusof, N.A.; Abdulla, J.; Shomiad, R.H. Strategies in the optimization of DNA hybridization conditions and its role in electrochemical detection of dengue virus (DENV) using response surface methodology (RSM). *RSC Adv.* **2023**, *13*, 18748–18759. [CrossRef]
22. Kumar, S.; Sidhu, H.K.; Paul, A.K.; Bhardwaj, N.; Thakur, N.S.; Deep, A. Bioengineered multi-walled carbon nanotube (MWCNT) based biosensors and applications thereof. *Sens. Diagn.* **2023**, *2*, 1390–1413. [CrossRef]
23. Speranza, G. The Role of Functionalization in the Applications of Carbon Materials: An Overview. *C* **2019**, *5*, 84. [CrossRef]

24. Moustakim, H.; Mohammadi, H.; Amine, A. Electrochemical DNA Biosensor Based on Immobilization of a Non-Modified ssDNA Using Phosphoramidate-Bonding Strategy and Pencil Graphite Electrode Modified with AuNPs/CB and Self-Assembled Cysteamine Monolayer. *Sensors* **2022**, *22*, 9420. [CrossRef] [PubMed]
25. Xu, P.; Wang, J.; Xu, Y.; Chu, H.; Shen, H.; Zhang, D.; Zhao, M.; Liu, J.; Li, G. Binding modes and interaction mechanism between different base pairs and methylene blue trihydrate, aquantum mechanics study. *Adv. Struct. Bioinform.* **2015**, 187–203.
26. Wang, L.; Liao, X.; Ding, Y.; Gao, F.; Wang, Q. DNA biosensor based on a glassy carbon electrode modified with electropolymerized Eriochrome Black T. *Microchim. Acta* **2014**, *181*, 155–162. [CrossRef]
27. Callison, S.A.; Hilt, D.A.; Boynton, T.O.; Sample, B.F.; Robison, R.; Swayne, D.E.; Jackwood, M.W. Development and evaluation of a real-time Taqman RT-PCR assay for the detection of infectious bronchitis virus from infected chickens. *J. Virol. Methods* **2006**, *138*, 60–65. [CrossRef] [PubMed]
28. Nidzworski, D.; Wasilewska, E.; Smietanka, K.; Szewczyk, B.; Minta, Z. Detection and differentiation of Newcastle disease virus and influenza virus by using duplex real-time PCR. *Acta Biochim. Pol.* **2013**, *60*, 475–480. [CrossRef]
29. Ghica, M.E.; Pauliukaite, R.; Fatibello-Filho, O.; Brett, C.M. Application of functionalised carbon nanotubes immobilised into chitosan films in amperometric enzyme biosensors. *Sens. Actuators B Chem.* **2009**, *142*, 308–315. [CrossRef]
30. Hnatow, L.L.; Keeler, C.L., Jr.; Tessmer, L.L.; Czymmek, K.; Dohms, J.E. Characterization of MGC2, a Mycoplasma gallisepticum cytadhesin with homology to the Mycoplasma pneumoniae 30-kilodalton protein P30 and Mycoplasma genitalium P32. *Infect. Immun.* **1998**, *66*, 3436–3442. [CrossRef]
31. Zhao, Y.; Kong, C.; Cui, X.; Cui, H.; Shi, X.; Zhang, X.; Hu, S.; Hao, L.; Wang, Y. Detection of infectious laryngotracheitis virus by real-time PCR in naturally and experimentally infected chickens. *PLoS ONE* **2013**, *8*, e67598. [CrossRef]
32. Siddiquee, S.; Yusof, N.A.; Salleh, A.B.; Tan, S.G.; Bakar, F.A. Electrochemical DNA biosensor for the detection of Trichoderma harzianum based on a gold electrode modified with a composite membrane made from an ionic liquid, ZnO nanoparticles and chitosan, and by using acridine orange as a redox indicator. *Mikrochim. Acta* **2011**, *172*, 357–363. [CrossRef]
33. Bhuiyan, M.S.A.; Sarker, S.; Amin, Z.; Rodrigues, K.F.; Baka, A.M.S.A.; Saallah, S.; Siddiquee, S. Seroprevalence and molecular characterisation of infectious bronchitis virus (IBV) in broiler farms in Sabah, Malaysia. *J. Vet. Med. Sci.* **2023**, *10*, e1153. [CrossRef]
34. Bhuiyan, M.S.A.; Ringgit, G.; Amin, Z.; Bakar, A.M.S.A.; Saallah, S.; Shaarani, S.M.; Siddiquee, S. Optimizing electrochemical DNA biosensors for the detection of avian infectious bronchitis virus. Malays. *J. Microbiol.* **2023**, *19*, 651–663.
35. Yang, Y.; Yang, D.; Shao, Y.; Li, Y.; Chen, X.; Xu, Y.; Miao, J. A label-free electrochemical assay for coronavirus IBV H120 strain quantification based on equivalent substitution effect and AuNPs-assisted signal amplification. *Mikrochim. Acta* **2020**, *187*, 624. [CrossRef] [PubMed]
36. Weng, X.; Neethirajan, S. Immunosensor based on antibody-functionalized MoS 2 for rapid detection of avian coronavirus on cotton thread. *IEEE Sens. J.* **2018**, *18*, 4358–4363. [CrossRef]
37. Liu, I.L.; Lin, Y.C.; Lin, Y.C.; Jian, C.Z.; Cheng, I.C.; Chen, H.W. A novel immune-chromatographic strip for antigen detection of avian infectious bronchitis virus. *Int. J. Mol. Sci.* **2019**, *20*, 2216. [CrossRef]
38. Nordin, N.; Yusof, N.A.; Radu, S.; Hushiarian, R. Development of an Electrochemical DNA Biosensor to Detect a Foodborne Pathogen. *J. Vis. Exp.* **2018**, *136*, e56585.
39. Wang, Q.; Zhang, B.; Lin, X.; Weng, W. Hybridization biosensor based on the covalent immobilization of probe DNA on chitosan–mutiwalled carbon nanotubes nanocomposite by using glutaraldehyde as an arm linker. *Sens. Actuators B Chem.* **2011**, *156*, 599–605. [CrossRef]
40. Zhao, W.R.; Kang, T.F.; Lu, L.P.; Cheng, S.Y. Electrochemical magnetic imprinted sensor based on MWCNTs@CS/CTABr surfactant composites for sensitive sensing of diethylstilbestrol. *J. Electroanal. Chem.* **2018**, *818*, 181–190. [CrossRef]
41. Shalauddin, M.; Akhter, S.; Bagheri, S.; Karim, M.M.A.; Kadri, N.A.; Basirun, W. Immobilized copper ions on MWCNTs-Chitosan thin film, Enhanced amperometric sensor for electrochemical determination of diclofenac sodium in aqueous solution. *Int. J. Hydrogen Energy* **2017**, *42*, 19951–19960. [CrossRef]
42. Markegard, C.B.; Gallivan, C.P.; Cheng, D.D.; Nguyen, H.D. Effects of concentration and temperature on DNA hybridization by two closely related sequences via large-scale coarse-grained simulations. *J. Phys. Chem. B* **2016**, *120*, 7795–7806. [CrossRef] [PubMed]
43. Nimse, S.B.; Song, K.; Sonawane, M.D.; Sayyed, D.R.; Kim, T. Immobilization techniques for microarray, challenges and applications. *Sensors* **2014**, *14*, 22208–22229. [CrossRef] [PubMed]
44. Benvidi, A.; Rajabzadeh, N.; Mazloum-Ardakani, M.; Heidari, M.M. Comparison of impedimetric detection of DNA hybridization on chemically and electrochemically functionalized multi-wall carbon nanotubes modified electrode. *Sens. Actuators B Chem.* **2015**, *207*, 673–682. [CrossRef]
45. Hassan, R.A.; Heng, L.Y.; Tan, L.L. Novel DNA biosensor for direct determination of carrageenan. *Sci. Rep.* **2019**, *9*, 6379. [CrossRef]

46. Kusnin, N.; Yusof, N.A.; Abdullah, J.; Sabri, S.; Mohammad, F.; Mustafa, S.; Al-Lohedan, H.A. Electrochemical sensory detection of Sus scrofa mtDNA for food adulteration using hybrid ferrocenylnaphthalene diimide intercalator as a hybridization indicator. *RSC Adv.* **2020**, *10*, 27336–27345. [CrossRef]
47. Ali, M.R.; Bacchu, M.S.; Setu, M.A.A.; Akter, S.; Hasan, M.N.; Chowdhury, F.T.; Khan, M.Z.H. Development of an advanced DNA biosensor for pathogenic Vibrio cholerae detection in real sample. *Biosens. Bioelectron.* **2021**, *188*, 113338. [CrossRef]
48. Moarefdoust, M.M.; Jahani, S.; Moradalizadeh, M.; Motaghi, M.M.; Foroughi, M.M.A. DNA Biosensor Based on a Raspberry-like Hierarchical Nanostructure for the Determination of the Anticancer Drug Nilotinib. *ChemistryOpen* **2022**, *11*, e202100261. [CrossRef]
49. Nordin, N.; Yusof, N.A.; Abdullah, J.; Radu, S.; Hushiarian, R. A simple, portable, electrochemical biosensor to screen shellfish for Vibrio parahaemolyticus. *AMB Express* **2017**, *7*, 41. [CrossRef]
50. López-Vidriero, I.; Godoy, M.; Grau, J.; Peñuelas, M.; Solano, R.; Franco-Zorrilla, J.M. DNA features beyond the transcription factor binding site specify target recognition by plant MYC2-related bHLH proteins. *Plant Commun.* **2021**, *2*, 100232. [CrossRef]
51. Iyuke, S.; Ntombenhle-Hlongwane, G.; Dodoo-Arhin, D.; Wamwangi, D.; Daramola, M.O.; Moothi, K. DNA hybridisation sensors for product authentication and tracing, State of the art and challenges. *S. Afr. J. Chem. Eng.* **2019**, *27*, 16–34.
52. Doğru, E.; Erhan, E.; Arikan, O.A. Investigation of Dilution Agent Effect onto Interactions Between Methylene Blue and DNA using Carbon Fiber Based DNA Biosensor. *J. New Mater. Electrochem. Syst.* **2017**, *20*, 65.
53. Campos-Ferreira, D.S.; Nascimento, G.A.; Souza, E.V.; Souto-Maior, M.A.; Arruda, M.S.; Zanforlin, D.M.; Lima-Filho, J.L. Electrochemical DNA biosensor for human papillomavirus 16 detection in real samples. *Anal. Chim. Acta* **2013**, *804*, 258–263. [CrossRef]
54. Ortega-Zamora, C.; Jiménez-Skrzypek, G.; González-Sálamo, J.; Mazzapioda, L.; Navarra, M.A.; Gentili, A.; Hernández-Borges, J. Extraction of Emerging Contaminants from Environmental Waters and Urine by Dispersive Liquid–Liquid Microextraction with Solidification of the Floating Organic Droplet Using Fenchol, Acetic Acid Deep Eutectic Mixtures. *ACS Sustain. Chem. Eng.* **2022**, *10*, 15714–15725. [CrossRef]
55. Jamaluddin, R.Z.A.R.; Tan, L.L.; Chong, K.F.; Heng, L.Y. An electrochemical DNA biosensor fabricated from graphene decorated with graphitic nanospheres. *Nanotechnology* **2020**, *31*, 485501. [CrossRef]
56. Bohari, N.A.; Siddiquee, S.; Saallah, S.; Misson, M.; Arshad, S.E. Optimization and analytical behavior of electrochemical sensors based on the modification of indium tin oxide (ITO) using PANI/MWCNTs/AuNPs for mercury detection. *Sensors* **2020**, *20*, 6502. [CrossRef]
57. Ahuja, S.; Kumar, M.S.; Nandeshwar, R.; Kondabagil, K.; Tallur, S. Longer amplicons provide better sensitivity for electrochemical sensing of viral nucleic acid in water samples using PCB electrodes. *Sci. Rep.* **2022**, *12*, 8814. [CrossRef]
58. Smith, M.; Withnall, R.; Anastasova, S.; Gil-Rosa, B.; Blackadder-Coward, J.; Taylor, N. Developing a multimodal biosensor for remote physiological monitoring. *BMJ Mil. Health* **2023**, *169*, 170–175. [CrossRef] [PubMed]
59. Liu, X.; Liu, J. Biosensors and sensors for dopamine detection. *View* **2021**, *2*, 20200102. [CrossRef]
60. Li, H.; Wan, C.; Wang, Z.; Tan, J.; Tan, M.; Zeng, Y.; Guo, X. Rapid diagnosis of duck Tembusu virus and goose astrovirus with TaqMan-based duplex real-time PCR. *Front. Microbiol.* **2023**, *14*, 1146241. [CrossRef]
61. Patel, S.A.; Thompson, N.G.; Nguyen, T.T. Electrochemical DNA biosensors for viral diagnostics. *ACS Omega* **2021**, *6*, 7123–7132.